Size determination of a chain in a bad solvent by intensity light scattering comparison with a good solvent state

S. Luzzati,* M. Adam and M. Delsanti
Service de Physique des Solides et de Résonance Magnétique, CEN-Saclay, 91191 Gif-sur-Yvette Cedex, France
(Received 15 July 1985; revised 23 September 1985)

The form factor of $P(\theta)$ of linear atactic polystyrene in cyclohexane ($M_w = 6.77 \times 10^6$) has been studied as a function of temperature from 4.3°C above to 3.9°C below the theta temperature. Changes of the polymer chain configuration with the quality of the solvent are clearly reflected in the range of validity of the approximation $P(\theta)^{-1} = 1 + (qR_g)^2/3$, generally used to determine the radius of gyration R_g. The highest value of $(qR_g)^2$ to which the approximation is valid decreases significantly on passing from the good solvent to the bad solvent condition.

(Keywords: light scattering; polymer configuration; bad solvent; chain size determination)

INTRODUCTION

The chain configuration of flexible linear polymers in dilute solution depends on the quality of the solvent. In a theta solvent segment–segment and segment–solvent interactions are equal in strength and chains can be fairly well represented as gaussian coils that obey random flight statistics. When the theta condition no longer holds, interactions cease to be balanced; in a good solvent there is coil expansion and in a bad solvent, coil contraction. The contraction as the solvent becomes poorer is represented by theoretical models[1] as a collapse of the single chain, which passes from coiled to globular configuration. This change of configuration is quite abrupt for polymers of high molecular weight and it is often described as a phase transition (coil–globule transition).

Much experimental research relates to the good solvent condition, whereas the bad solvent condition has not been so widely studied[1,2] because measurements are somewhat more difficult than in a good solvent. To observe the chain in a collapsed state, very high molecular weights are needed, but there is an upper limit to molecular weight owing to polymer polydispersity, which increases with molecular weight and may drastically influence the experiment. To observe single chain behaviour a very low concentration is required; it is difficult to find a good compromise between dilution and results with a reasonable signal-to-noise ratio. In elastic and quasi-elastic light scattering with chains of high molecular weight an acceptable signal-to-noise ratio is maintained to a very high dilution level. A polymer–solvent pair often used to model the bad solvent conditions is polystyrene–cyclohexane; for this system the theta temperature, θ_t, is 35°C, the temperature at which the second virial coefficient of the osmotic pressure vanishes[3]. The solvent quality becomes poorer when the temperature falls below θ_t. The variation with temperature of the chain dimension, or chain expansion, was widely studied above, but rarely below, θ_t. It has clearly been shown experimentally[4] that for polystyrene–cyclohexane the temperature has only a perturbative effect in the temperature zone called the theta domain, $|(T-\theta_t)/\theta_t|\sqrt{M} \leqslant 10$; but has an important effect out of the theta domain, i.e. $|(T-\theta_t)/\theta_t|\sqrt{M} > 10$. For $T > \theta_t$ as well as for $T < \theta_t$, the expansion factors depend on $|(T-\theta_t)/\theta_t|\sqrt{M}$, which is the reduced temperature variable. For $T > \theta_t$, the chains can be either gaussian or swollen, depending on molecular weight.

In the good solvent conditions, Noda *et al.*[5] have measured by elastic light scattering the form factor $P(\theta)$ of highly monodisperse polystyrene chains of very high molecular weight ($M > 10^6$) in toluene. Their results could not be made to conform with existing theories. This work represents an experimental contribution to the study of the form factor $P(\theta)$ in a bad solvent.

THEORETICAL BACKGROUND

It is well known that information on dimensions and chain configurations can be obtained through elastic light scattering experiments[6]. For a very dilute solution of monodisperse chains of concentration c (g cm^{-3}), with dimensions larger than $\lambda/30$ (λ is the incident wavelength in the medium), the excess scattered intensity, $I(\theta)$, depends on the scattering angle, θ, in the medium. This angular anisotropy, measured experimentally as $I(\theta)_{c\to 0}/I(\theta\to 0)_{c\to 0}$, is caused by intraparticle interference and expressed through the form factor $P(\theta)$:

$$P(\theta) = \frac{1}{N^2}\sum_{ij}\left\langle \frac{\sin qr_{ij}}{qr_{ij}} \right\rangle \qquad (1)$$

where N is the number of statistical segments of the chain, r_{ij} is the distance between segment i and segment j and q is

* Present address: Dipartimento di Chimica, Politecnico di Milano, Piazza L. da Vinci 32, 20133 Milano, Italy.

0032-3861/86/060834-05$03.00

the transfer vector, defined as $q=4\pi/\lambda \sin(\theta/2)$. Equation (1) is the intraparticle interference averaged over all possible orientations of the chains, on the assumption that there is no preferential orientation (the brackets indicate averaging related to changes in shape). For $qR_g<1$ it can be easily shown that $P(\theta)$ depends only on the mean square radius of gyration R_g^2, and is approximated usually to[7]:

$$P^{-1}(\theta)=1+\frac{q^2R_g^2}{3} \qquad (2)$$

For $qR_g>1$, equation (1) must be solved exactly, introducing a model for the distribution function $W(r_{ij})$ of the intersegmental distances.

$P(\theta)$ was calculated for gaussian coils by Debye[8], who assumed for $W(r_{ij})$ a gaussian distribution with a mean square intersegmental distance $r_{ij}^2 \sim |i-j|$, where $|i-j|$ is the number of statistical segments between segment i and segment j:

$$P(\theta)=2(qR_g)^{-4}(e^{-(qR_g)^2}+(qR_g)^2-1) \qquad (3)$$

This function fits well with the experimental results for theta solvents[9].

No good model is presently available to fit the experiments obtained with linear polymers in a good solvent[5]. A model has been proposed[10-12] in which the gaussian behaviour of $W(r_{ij})$ is maintained and a parameter, v, is introduced into the expression for the mean square intersegmental distance: $\langle r_{ij}^2\rangle \sim |i-j|^{2v}$ (for a theta solvent $v=1/2$, for a good solvent $v\approx 3/5$). From now on we will call this model the P model.

Other calculations have been done using the blob model[13]: the chain configuration is gaussian up to N_c statistical segments, i.e. inside the blob $\langle r_{ij}^2\rangle \sim |i-j|$, and it has an excluded volume behaviour for $|i-j|>N_c(\langle r_{ij}^2\rangle \sim |i-j|^{1.2})$. These two models are extended in the bad solvent regime using $v=1/3$.

Recently, Allegra and Ganazzoli[14,15] proposed for the collapsed coil a theory where they maintained a gaussian intersegmental distribution function and ascribed two-regime behaviour to the chain. For $|i-j|<N_c$, $\langle r_{ij}^2\rangle$ is proportional to $|i-j|$, as in the blob model, while for $|i-j|>N_c$, $\langle r_{ij}^2\rangle$ is equal to a constant that depends only on molecular weight and temperature.

If the length probed by the experiment is shorter than the size of the blob, Allegra and blob models lead to a $P(\theta)$ that tends to the Debye function, while if the length probed by the experiment is larger than the size of the blob the Allegra model predicts a $P(\theta)$ that deviates more from the Debye function than do the P model and the blob model. This can be easily shown by the value of amplitude of the third term in the expansion of $P^{-1}(\theta)$:

$$P^{-1}(\theta)=1+(qR_g)^2/3+A(qR_g)^4+\ldots$$

where A = 0.028 for the Debye function, A = 0.041 for the P model, A = 0.078 for the Allegra model.*

Before presenting the experimental results, it is worth while mentioning some of the basic equations that will be used to analyse the measurements. The Rayleigh ratio $R(\theta)$ of a dilute solution of monodisperse polymers can be written as:

$$KcR(\theta)=1/MP(\theta)+2A_2Q(\theta)c$$

where $P(\theta)$ and $Q(\theta)$ are the intramolecular and intermolecular interference contributions, and A_2 represents the second virial coefficient of the osmotic pressure. For incident polarized light the constant K_c is equal to $4\pi^2 n_{\lambda_0}^2(\partial n/\partial c)^2/\lambda_0^4 N_a$, where λ_0 is the incident wavelength in vacuum, n_{λ_0} is the solvent index of refraction, $\partial n/\partial c$ is the incremental refractive index and N_a is the Avogadro number.

Experimentally $R(\theta)$ is determined by measuring the intensity I_b scattered by a pure benzene sample under the same experimental conditions under which $I(\theta)$ is measured: $R(\theta)=R_bI(\theta)/I_b$, where R_b is the Rayleigh ratio of benzene. Generally at high values of q^{-1} with respect to the range of interparticle interactions, the Zimm single-contact approximation[16] is valid and $Q(\theta)=1$. In this case a linear extrapolation to $c=0$ gives $P(\theta)$.

For $qR_g<1$, equation (2) is valid, so that:

$$Kc/R(\theta)=[1+(qR_g)^2/3]/M+2A_2c \qquad (4)$$

and A_2, R_g and M can be determined*.

Since the measurements were performed with a spectrometer designed in our laboratory, first of all the apparatus will be described and its specification given. Experimental results will then be presented.

EXPERIMENTAL

Spectrometer

The spectrometer is designed for both elastic and quasi-elastic light scattering experiments. The apparatus was tested on polystyrene–benzene solutions as described later.

A schematic diagram of the apparatus is shown in *Figure 1*: a laser beam (coherent CR2 argon laser, $\lambda_0=4880$ Å) is reflected by a mirror through two diaphragms, D_1 and D_2, that clean the beam and ensure that it is parallel to the optical table. To control the incident intensity a fraction of the beam is deviated by a thin glass plate, B.S., to a photodiode, Di. The beam is focused on the centre of the sample cell, C, by a lens of focal length 200 mm, L_1; a 150 μm diameter pinhole, D_3, and a lens of focal length 60 mm, L_2, project the image of the scattering volume on to the photocathode of a EMI 9863/A350 photomultiplier, P.M., and a pair of vertical and horizontal slits, F, define it. Just before the photocathode there is an interferential filter centred at 4880 Å. The collection optics and the photomultiplier are fixed to a rotating arm supported at one edge by a Microcontrole goniometer with angular precision of 0.01°; the optical elements and the photomultiplier can be adjusted three-dimensionally. The signal from the photomultiplier is digitalized by an A.T.N.E. amplifier–discriminator, Dis., and sent to a 1 bit, 24 channel Malvern K7023 correlator. The outputs of the correlator and of the Fluke 8810A digital multimeter (M.V.) that measures the output of the photodiode are sent to

* Allegra, P., private communication

* In a real experiment the polymer is not completely monodisperse so that the Z average of the square of the radius of gyration and the weight average of the molecular weight are the measured quantities.

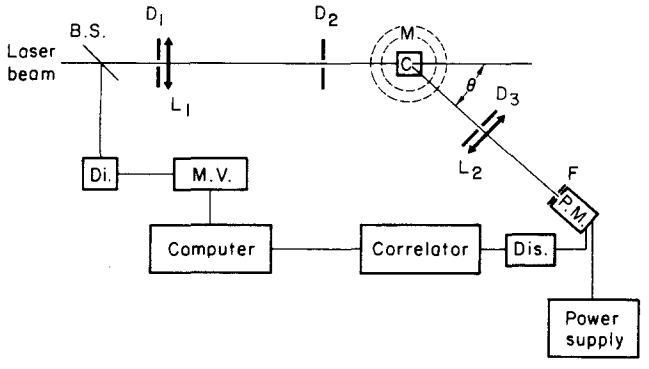

Figure 1 Block diagram of the spectrometer. D_1, D_2, diaphragms; D_3, pinhole; B.S., thin glass plate; Di., photodiode; L_1, L_2, lenses; P.M., photomultiplier; F, slits; Dis., amplifier–discriminator; C, sample cell; M, goniometer, M.V., digital multimeter

HP 9820A on-line computer. The total number of photocounts normalized by the incident intensity was determined.

The sample cell is held at the centre of the goniometer and is surrounded by an index matching and temperature-controlled bath consisting of a glass cylinder, with optical polished surfaces, filled with tetrachloroethylene and clamped to a stainless steel block. The stainless steel block has the bottom thermally isolated by a Perspex disk and is fixed to an aluminium base, screwed to the optical table and to the goniometer.

All the parts were carefully centred to ensure cylindrical symmetry of the apparatus. The centricity of the index matching cylinder was checked by optical methods. Hellma sample cells of optical glass of cylindrical and rectangular shape, with a 10 mm and 20 mm optical path, respectively, were used. The cells were aligned along the axis of the index matching cylinder, and held at the top.

To facilitate optical alignment, the index matching bath as well as the collection optics elements were removable. The accuracy of the optical alignment was checked by determining to what extent the intensity scattered by pure benzene was independent of scattering angle; a typical plot of the reduced intensity $I_b(\theta)\sin\theta/I_b(90°)$ *versus* θ is shown in *Figure 2*. With rectangular cells measurements have a typical error of $\pm 2\%$ for angles greater than 13°. With cylindrical cells the error reduces to $\pm 1\%$ for $\theta > 20°$. At angles smaller than 13° and 20° with rectangular and cylindrical cells respectively, the increase of the reduced intensity is mainly due to stray light. For these experiments careful analysis of the lower q region was required; as the solute scatters at least 4 times more than benzene at $\theta = 0°$, it was advantageous to use rectangular cells, although this required making an angle correction because solutions do not have the same index of refraction as the index matching bath.

Sample preparation

Polystyrene–cyclohexane or polystyrene–benzene samples were prepared at different concentrations with polystyrene fractions (Toya Soda), whose characteristics are given in *Table 1*. The solvent was high quality cyclohexane or Normapur benzene. Usually, 50 cm^3 of solution was prepared by weighing at a concentration $w \approx 10^{-3}$ g g^{-1} and was kept in an oven for 3 weeks at 45°C to let the polystyrene dissolve properly. Then by dilution different solutions were prepared directly in the sample cells, which were left at least another week in the oven before use.

The solutions were not filtered but the cells and the glassware kit were cleaned in chromic acid and rinsed with solvent. In this work, filtration may involve more difficulties than advantages; the cyclohexane and benzene used were dust-free and with the low polymer concentration studied it was enough to let dust sediment in the cells for at least one week and to handle them gently, without shaking. When these procedures were used there was no sparkle at low scattering angle and experimental results were reproducible after several months.

Temperature control and range of temperature investigated for polystyrene–cyclohexane solutions

The index matching bath was thermostatically controlled from the bottom by a stainless steel block in which water was circulated from an external regulated bath. The system allowed temperature control to ± 0.1°C from 25 to 42°C; at the precision of temperature reading (0.05°C), no gradient in the sample cell can be detected.

Before starting the experiment the coexistence curve was located to fix the lowest temperature limit. Cooling from θ_t step by step, the scattered intensity at one angle (30°) was measured for the highest (7.36×10^{-4} g g^{-1}) and lowest (4.5×10^{-5} g g^{-1}) concentrations; the intensity increased abruptly at 30.5°C and 30°C, respectively.

A measurement made at 30.3°C with a solution of $w = 4.5 \times 10^{-5}$ g g^{-1} revealed the influence of the coexistence curve. Even if there was not, during the 4 h of measurement, any evidence of macroscopic phase separation (the intensity was stable in time and speckles at low scattering angles did not appear) the plot of $wI_b/I(\theta)$ versus q^2 decreased sharply at low angles ($\theta \leqslant 35°$). This observation has been recently reported for polystyrene in cyclohexane ($10^4 \leqslant M_w \leqslant 18 \times 10^4$), by Einaga *et al.*[17], who suggested that it may reflect the occurrence of microphase separations that trigger a macroscopic one. Thus it was decided to maintain the solutions 1°C above the demixing temperature. The measurements were made at the following temperatures: 39.3°C, 35.0°C, 32.0°C, 31.1°C. The highest and the lowest temperatures correspond to reduced temperature variables $(T-\theta_t)/\theta_t\sqrt{M}$ of 36 and -33, respectively; at these two temperatures the configuration of the polymer of $M_w = 6.77 \times 10^6$ is certainly not gaussian because the two reduced temperatures are bigger than the reduced temperature relating to the theta domain $|(T-\theta_t)\theta_t|\sqrt{M} < 10$).

Test of the apparatus

The reliability of the apparatus was first determined by making measurements on two different monodisperse polystyrene–benzene solutions at 20°C; the characteris-

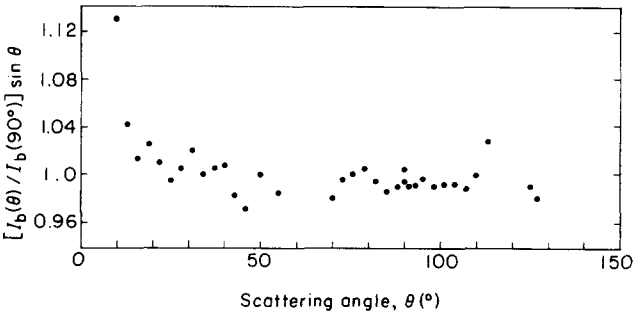

Figure 2 Variation of the reduced intensity of the light scattered by benzene corrected for the scattering volume (rectangular cell) as a function of the scattering angle

Table 1 Characteristics of the samples used and range of weight fraction w(g g^{-1}) within which the experiments were performed

	M_w[a]	M_w/M_n[b]	w (g g^{-1})
Benzene	4.39×10^4	1.01	10^{-3}–10^{-2}
	1.26×10^6	1.04	10^{-4}–10^{-3}
Cyclohexane	6.77×10^6	1.14	0.45–7.36×10^{-4}

[a] M_w, weight average molecular weight
[b] M_w/M_n, index of polydispersity

tics of the solutions are given in *Table 1*. The quotient $wI_b/I(\theta)$ had been analysed using the abovementioned double extrapolation procedure (see equation (4)). The ratio of our origins $wI_b/I(\theta)$ as $w\to0$ and $\theta\to0$ corresponds, with a 5% error, to the ratio of the two $M_w$values given by Toyo Soda. Then, assuming the M_w values to be correct, the Rayleigh ratio of benzene was calculated to be $R_b=3.73\times10^{-5}$ cm^{-1}, in good agreement with literature data[18–20]. For benzene $d_{20°C}=0.8794$ g cm^{-3} (ref. 21), $n_{4880Å}=1.514$ and $\partial n/\partial c=0.1076$ cm^3 g^{-1} (refs. 6 and 22).

For polystyrene–cyclohexane samples we find $M_w=6.52\times10^6$, in good agreement with the Toyo Soda value (6.77×10^6); for cyclohexane $n_{35°C}=1.423$, $\partial n/\partial c=0.1744$ cm^3 g^{-1} (n and $\partial n/\partial c$ values are deduced from refs. 6 and 22 using a Cauchy dispersion), $K=7.1243\times10^{-7}$ cm^2 mol g^{-2}.

EXPERIMENTAL RESULTS AND DISCUSSION

Measurements were generally made at each temperature and concentration by varying the scattering angle from 10° to 140°, taking about 70–75 different angles, which were selected irregularly to avoid systematic errors. In *Figure 3*, $Kc/R(\theta)$ is plotted as a function of $\sin^2\theta/2$ for $\theta<90°$ for the following experimental conditions: $w=4.504\times10^{-5}$ (g g^{-1}) for $T=39.3$°C, $w=1.15\times10^{-4}$ (g g^{-1}) for $T=35$°C and 31.1°C. Unbroken graphs show the least squares best fit using equation (2) and the measurements performed at low $\sin^2\theta/2$; the corresponding radii of gyration determined are listed in *Table 2*.

In fact these plots, and the equivalent one for $T=32.5$°C and $w=1.15\times10^{-4}$ (g g^{-1}) (not represented in *Figure 3*) were used without extrapolating to zero w, and R_g, M_w and $P(\theta)$ were calculated. Extrapolating to $w=0$ at each angle has the only effect of adding some noise to the plots of *Figure 3*. However confidence can be placed in this procedure because

(i) the $2MA_2c$ terms, where A_2 is calculated from the concentration dependence of $Kc/R(\theta)|_{\theta\to0}$ on c, are in the case of *Figure 3* less than 2%;

(ii) the intercepts on the axis of ordinates of $Kc/R(\theta)$ in *Figure 3* are within 3.6×10^{-2}, independent of the temperature ($Kc/R(\theta)|_{\theta\to0}=1.454\times10^{-7}$ at 39.3°C, 1.543×10^{-7} at 35°C, 1.565×10^{-7} at 32°C, 1.576×10^{-7} at 31.1°C).

At the theta temperature the determined radius of gyration ($R_g=748\pm22$ Å) is in good agreement with those reported in the literature ($R_g=0.29\sqrt{M_w}$ (Å))[23]. In *Figure 4* one can see that the form factor $P(\theta)$ fits well with the Debye function of equation (3). At $T=39.3$°C and $T=31.1$°C, $P(\theta)$ deviates from the Debye function in opposite directions (see *Figure 4*). Just to have a visual guide to the change from the good solvent condition to the bad solvent condition the $P(\theta)$ calculated with the P model using $\nu=3/5$ and $\nu=1/3$ has been plotted in an inset of *Figure 4*. For $T=39.3$°C, an experimental form factor $P(\theta)$ between the Debye function and the

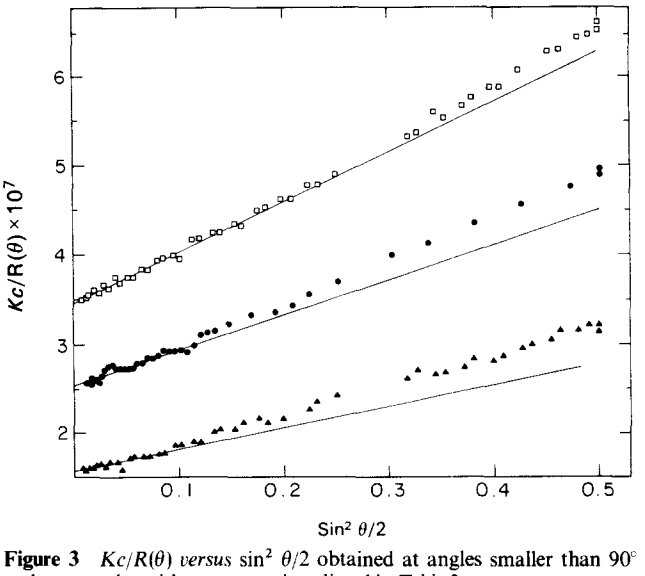

Figure 3 $Kc/R(\theta)$ *versus* $\sin^2\theta/2$ obtained at angles smaller than 90° and on samples with concentrations listed in *Table 2* at temperatures: ▲, 31.1°C; ●, 35°C; □, 39.3°C. Graphs are the best least-squares fit to equation (2) of experimental points obtained at low scattering angles. Points ● and □ are displaced along the axis of ordinates by 1×10^{-7} and 2×10^{-7} respectively

Table 2

Temperature (°C)	$c\times10^5$[a] (g cm^{-3})	Radius of gyration R_g (Å)	$(qR_g)^2_{max}$[b]	A_2[c] (cm^2 mol^{-1} g^{-2})
39.3	3.42	921±27	1.1	2.5×10^{-5}
35.0	8.8	748±22	0.9	–
32.5	8.9	682±35	0.75	–[d]
31.1	8.91	586±21	0.63	-1.5×10^{-5}

[a] c, the lowest concentration at which experiments were performed, was deduced from the measured weight fraction by $c=dw$, where d, the solvent density, is calculated from $d=0.7977-9.59\times10^{-4}\,T$(°C)
[b] $(qR_g)^2_{max}$ represents the upper value of $(qR_g)^2$ for which the approximation of equation (2) is valid
[c] Second virial coefficient of the osmotic pressure
[d] The slope of $Kc/R(\theta)|_{\theta\to0}$ versus c was too small to evaluate A_2

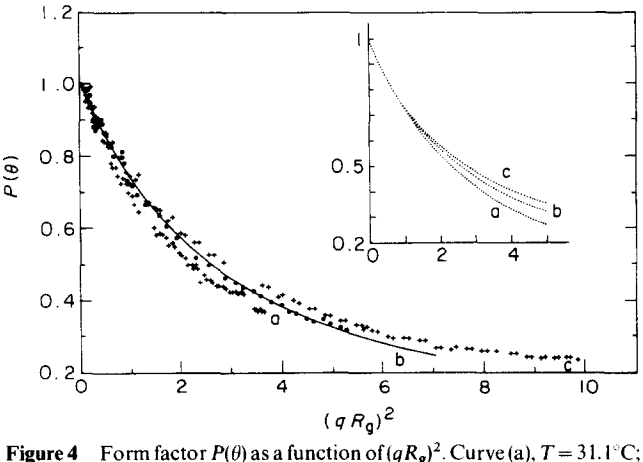

Figure 4 Form factor $P(\theta)$ as a function of $(qR_g)^2$. Curve (a), $T=31.1$°C; curve (b), $T=35$°C (full line corresponds to Debye function equation (3); curve (c), $T=39.3$°C. Within the inset is shown the graph of the theoretical form factor calculated with $\nu=1/3$ (curve a), $\nu=1/2$ (curve b) and $\nu=3/5$ (curve c) using the P model

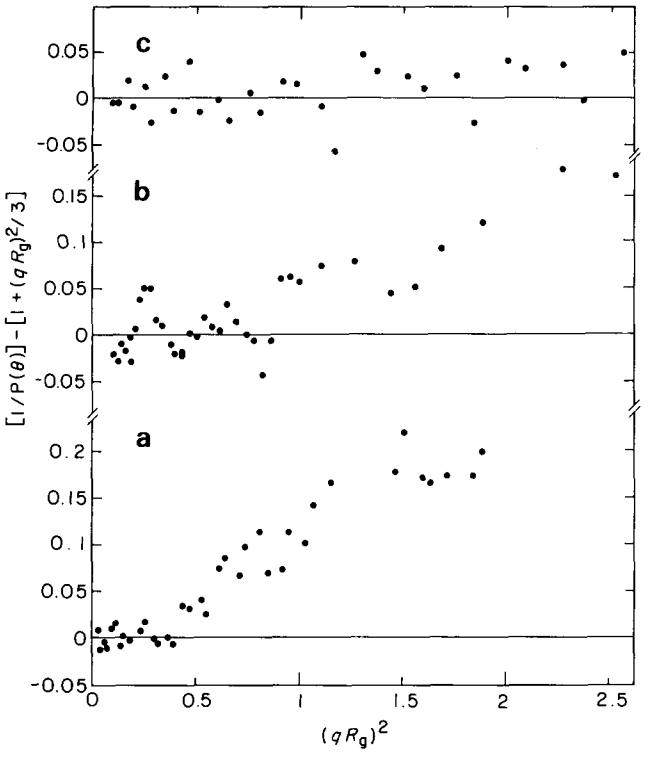

Figure 5 $[1/P(\theta)]-[1+(qR_g)^2/3]$ as a function of $(qR_g)^2$ for (a) 31.1°C; (b) 35°C; (c) 39.3°C

theoretical $P(\theta)$ with $\nu=3/5$, is found; this is in agreement with previous results[5]. For $T=31.1$°C, $P(\theta)$ has a more pronounced curvature in the range $1<(qR_g)^2<1.5$ than the P model with $\nu=1/3$. Unfortunately our comments on variations of $P(\theta)$ can be quantitative only. With our experimental conditions, at the lowest temperature, the maximum value of $(qR_g)^2$ is of the order of 5. The differences from the Debye function are just slightly greater than the experimental error. Nevertheless, it is not possible to fit the data to the Debye function by changing R_g within the error bar, the experimental $P(\theta)$ is always distorted by comparison.

The change in shape of $P(\theta)$ with temperature is unambiguously detected if the range of validity of equation (2) is studied. In *Figure 5* $[1/P(\theta)]-[1+(q^2R_g^2)/3]$ is plotted as a function of $(qR_g)^2$ for $T=39.3$°C, 35°C and 31.1°C, which allows determination of the range of $(qR_g)^2$ $(0<(qR_g)^2<(qR_g)^2_{max})$ where equation (2) is valid. $(qR_g)^2_{max}$ decreases with temperature, from 1.1 at 39.3°C to 0.63 at 31.1°C; $(qR_g)^2_{max}$ values are listed in *Table 2*—note that changing R_g within its error bar has no significant influence on the values of $(qR_g)^2_{max}$.

CONCLUSION

The form factor $P(\theta)$ of linear atactic polystyrene dissolved in cyclohexane has been studied as a function of the quality of the solvent. Polymer of $M_w=6.77\times10^6$ with index of polydispersity = 1.14 has been used and elastic light scattering measurements have been made for several concentrations ranging from $w=4.5\times10^{-5}$ g g^{-1} to 7.36×10^{-4} g g^{-1}. The temperature was varied from 4.3°C above to 3.9°C below the theta temperature, that is $((T-\theta_t)/\theta_t)\sqrt{M}=36$ and -33, respectively, the latter temperature being chosen to avoid the neighbourhood of the coexistence curve.

At the theta temperature the data can be well fitted to the form factor calculated by Debye for a gaussian coil. For $T>\theta_t$ and for $T<\theta_t$ the form factor varies in opposite directions. Although it is impossible to analyse quantitatively the changes of $P(\theta)$ in the whole qR_g range, there are some interesting hints to the behaviour of $P(\theta)$ in a bad solvent. Its curvature, for $(qR_g)^2\sim1.5$, is higher than that of the P model with $\nu=1/3$. The same kind of trend has been recently predicted by the model of Allegra and Ganazzoli. The approximation $P(\theta)^{-1}=1+(qR_g)^2/3$, normally used to calculate the radius of gyration, has to be used very carefully in the case of the bad solvent. The upper angular limit to this approximation, in terms of qR_g, decreases significantly on passing from the good solvent to the bad solvent condition.

ACKNOWLEDGEMENTS

The authors thank M. Labouise for technical assistance, and G. Allegra and F. Ganazzoli for helpful discussion. S.L. thanks the Italian National Research Council (CNR) and CEA for fellowships covering her stay in Saclay.

REFERENCES

1 Williams, C., Brochard, F. and Frish, H. L. *Ann. Rev. Phys. Chem.* 1981, **32**, 433 and references therein
2 Vidaković, P. Thesis Paris VI, 1983; Perzynski, R. Thesis Paris VI, 1984; Perzynski, R., Delsanti, M. and Adam, M. *J. Phys. (Paris)* 1984, **45**, 1765; Vidaković, P. and Rondelez, F. *Macromolecules* 1984, **17**, 418; Stepanek, P., Konak, C. and Sedlacek, B. *Macromolecules* 1982, **15**, 1214; Miyaki, Y. and Fujita, H. *Polym. J.* 1981, **13**, 749; Nishio, I., Swislow, G., Sun, S. T. and Tanaka, T. *Nature (Lond.)* 1982, **300**, 243
3 Strazielle, C. and Benoit, H. *Macromolecules* 1975, **8**, 203
4 Perzynski, R., Adam, M. and Delsanti, M. *J. Phys. (Paris)* 1982, **43**, 129; Cotton, J. P. Nierlich, M., Boué, F., Daoud, M., Farnoux, B., Jannink, G., Duplessix, R. and Picot, C. *J. Chem. Phys.* 1976, **65**, 1101
5 Noda, I., Imai, M., Kitano, T. and Nagasawa, M. *Macromolecules* 1983, **16**, 425
6 Huglin, M. B. 'Light Scattering from Polymer Solutions', Academic Press, London, 1972
7 Yamakaw, H. 'Modern Theory of Polymer Solutions', Harper & Row, New York, 1971
8 Debye, P. J. *J. Phys. Colloid. Chem.* 1947, **51**, 18
9 Kato, T., Katsuhiko, M., Noda, I., Fujimoto, T. and Nagasawa, M. *Macromolecules* 1970, **3**, 777
10 Peterlin, A. *J. Chem. Phys.* 1955, **23**, 2464
11 Ptitsyn, O. B. *Zh. Fiz. Khim.* 1957, **31**, 1091
12 Benoit, H. *C.R. Acad. Sci. Paris* 1957, **245**, 2244
13 Farnoux, B., Boué, F., Cotton, J. P., Daoud, M., Jannink, G., Nierlich, M. and de Gennes, P. G. *J. Phys. (Paris)* 1978, **39**, 77
14 Allegra, G. and Ganazzoli, F. *Macromolecules* 1983, **16**, 1311
15 Allegra, G. and Ganazzoli, F. *J. Chem. Phys.* 1985, **83**, 397
16 Zimm, B. H. *J. Chem. Phys.* 1948, **16**, 1093
17 Einaga, Y., Ohashi, S., Tong, Z. and Fujita, H. *Macromolecules* 1984, **17**, 527
18 Pike, E. R., Pomeroy, W. R. M. and Vaughan, J. M. *J. Chem. Phys.* 1975, **62**, 3188
19 Kaye, W. and McDaniel, J. B. *Appl. Optics* 1974, **13**, 1934
20 Cohen, G. and Eisenberg, H. *J. Chem. Phys.* 1965, **43**, 3881
21 Timmermans, J. 'Physico-chemical Constants of Pure Organic Compounds', Elsevier, Amsterdam, 1950
22 Miyaki, Y., Einaga, Y., and Fujita, H. *Macromolecules* 1978, **11**, 1180
23 Schmidt, M. and Burchard, W. *Macromolecules* 1981, **14**, 210